

Boundary Effects near the Superfluid Transition (BEST), an Experiment Proposed for the ISS

Guenter Ahlers*, Paul Finley†, Edgar Genio*, Kerry Kuehn*,
Feng-Chuan Liu†, Yuan-Ming Liu†, Sarabjit Mehta*, and Daniel Murphy*

*Department of Physics and Quantum Institute,
University of California, Santa Barbara, California 93106

†Jet Propulsion Laboratory, M/S 79-24

California Institute of Technology
4800 Oak Grove Drive, Pasadena, CA 91109

*Telephone: 805-893-3795; Email: guenter@stc.ucsb.edu

Abstract. We review the opportunities for microgravity measurements of the thermal resistivity $R(L, t)$ near the bulk superfluid-transition line $T_\lambda(P)$ of ^4He confined in cylindrical geometries with axial heat flow. A scaling function is used to estimate R as a function of the cylinder radius L and of the pressure P . These predictions are used to assess the effect of gravity on potential Earth-based measurements. Diameters $L \gtrsim 8 \mu\text{m}$ can only be investigated fully in micro-gravity. At higher pressures the gravity effect is larger. At 30 bar samples with $L \gtrsim 4 \mu\text{m}$ require micro-gravity. Modern thermometry has sufficient resolution to permit quantitative measurements of the finite-size effect for L as large as $50 \mu\text{m}$, the size chosen for the proposed ISS experiment BEST.

I. INTRODUCTION

An interesting issue in condensed-matter physics is the nature of the interface between solids and fluids. When the fluid is near a critical point, the boundary layer adjacent to the solid surface acquires a macroscopic thickness and the boundary influences significantly the average macroscopic properties of the system. In addition to these “surface” effects, a system confined in a finite geometry also exhibits “bulk” finite-size effects; both contributions are expected to be describable within the general context of finite-size scaling (Fisher, 1971) and by specific calculations based on the renormalization-group theory (RGT) (Dohm, 1993). We collectively refer to them as “finite-size effects”.

Experiments on *transport* properties in manifestly finite geometries are scarce. We only know of the data for the thermal resistivity R of Kahn and Ahlers (KA) (Kahn, 1995) for ^4He near the superfluid-transition temperature $T_\lambda(P)$ at SVP. Their sample was contained in the long, narrow tubes of a glass capillary array (GCA) (also known as micro-channel plates).¹ The tube radius L was $1 \mu\text{m}$. The major goal of the flight-definition project “Boundary Effects on transport properties and dynamic finite-size scaling near the Superfluid Transition line of ^4He ” (BEST) is to provide data for R over a wide range of L and P . Plans for this work will build upon the KA measurements and the assumption of finite-size scaling. The present paper describes the *expected* behavior of the system if it is *assumed* that finite-size

¹Glass capillary arrays with L from 1 to $50 \mu\text{m}$ are available commercially from Galileo Electro-Optics Corporation, Collimated Holes, Inc., and Hamamatsu Corp.

scaling is valid. One of the objective of the experiments will be to test this assumption. The other will be to provide detailed data for comparison with specific RGT calculations of $R(t, L)$ [$t \equiv 1 - T/T_\lambda(P)$].

II. THEORETICAL PREDICTIONS

Although scaling has been used for finite-size effects on static properties, there is at present *no* experimental foundation for its application to transport properties. Thus our work will provide the first test of finite-size scaling for the dynamics. For the cylindrical geometries, we take L to be equal to the cylinder radius. In analogy to static scaling arguments, we expect the relationship between $R(t, L)$ and $R(t) \equiv R(t, \infty)$ to be given by a function only of L/ξ , where

$$\xi = \xi_0 t^{-\nu} \quad (1)$$

with $\nu = 0.6705$ (Goldner, 1992) is the bulk correlation length above T_λ . Thus we write $R(t)$ in terms of $\xi(t)$ as

$$R(t) = R_0 \xi_0^{x/\nu} \xi^{-x/\nu} \quad (2)$$

and make the ansatz

$$R(t, L) = R(t) \tilde{F}(L/\xi) . \quad (3)$$

We find the scaling function

$$F(X) = (L/\xi_0)^{x/\nu} [R(t, L)/R_0] \quad (4)$$

with

$$X \equiv (L/\xi_0)^{1/\nu} |t| . \quad (5)$$

Equation 4 can be used to calculate $R(t, L)$ from $R(t)$ and L for any L .

III. NEED FOR MICRO-GRAVITY

One purpose of the planned work is to determine whether $F(X)$ is universal, *i.e.* independent of L and P . This will be possible only when data become available along several isobars over a significant range of L and of t . However, for large L the finite-size effects of interest occur very close to T_λ where the sample inhomogeneity due to the Earth's gravitational acceleration has a significant influence. This limits the range of L accessible on Earth.

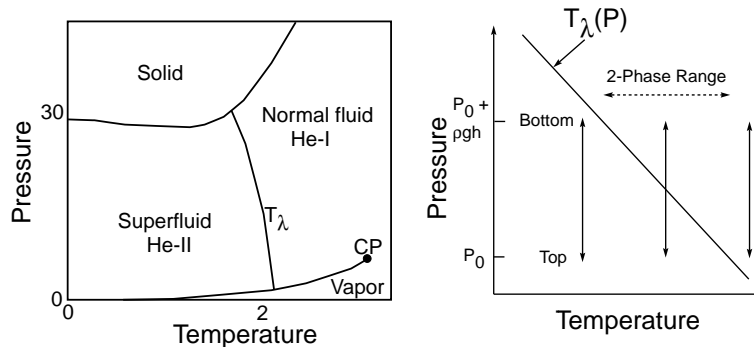


FIG. 1. Schematic phase diagram of ^4He , and an illustration of the gravity effect.

The gravity effect is illustrated in Fig. 1 in terms of the phase diagram of ${}^4\text{He}$. The λ line, along which the liquid undergoes a transition from a superfluid (He-II) to a normal (Navier-Stokes) liquid (He-I), extends from 2.176 K at vapor pressure (0.05 bar) to 1.763 K at the melting pressure (30.13 bar). The inhomogeneity induced by gravity (Ahlers, 1968 & 1991) is due to the hydrostatic pressure which varies with height in the liquid. This pressure variation has the effect of inducing a vertical spatial variation of $T_\lambda(P)$. This is illustrated in more detail in the right portion of Fig. 1. If the sample top is at a pressure $P = P_0$, then the bottom will be at $P = P_0 + \rho gh$ where ρ is the fluid density, g the gravitational acceleration, and h the sample height. Over this pressure range $T_\lambda(P)$ varies significantly. The parameter $\beta \equiv -(\partial T/\partial z)_\lambda$ is given by

$$\beta = -\rho g(\partial T/\partial P)_\lambda \quad (6)$$

and provides a quantitative measure of the severity of the gravity effect. Values of $\beta(P)$, in $\mu\text{K}/\text{cm}$, are given in Fig. 2. One sees that, for a typical sample of size 1 cm at SVP, one has a two-phase region over a temperature interval of 1.27 μK . Thus it is not possible to approach the transition more closely on average than within a μK or so. At higher pressures $\beta(P)$ increases. At 30 bar the two-phase region for a sample of a given height would be wider by a factor of 2.5. Of course the effect of gravity on the average measured properties extends well beyond the two-phase region.

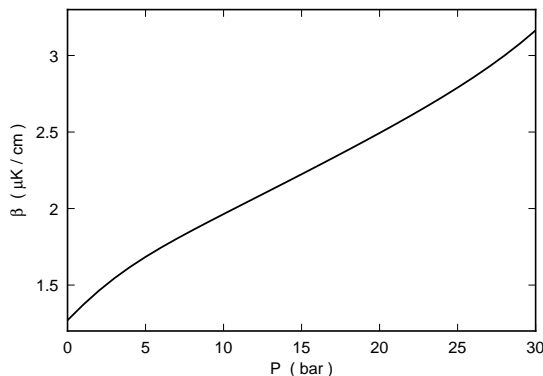


FIG. 2. The width β per cm of sample height of the temperature range of isothermal coexistence of He-I and He-II as a function of the pressure P . The values are for the gravitational acceleration on the Earth’s surface.

IV. ANALYSIS OF EXISTING DATA

A. Resistivity of Bulk ${}^4\text{He}$

An evaluation of the finite-size $R(t, L)$ requires an accurate knowledge of the bulk resistivity. We use the data by Tam and Ahlers (Tam, 1985) for their “Cell F” (TA) because they cover a very wide range of reduced temperatures, and because they are the only set we know of which covers several isobars in addition to saturated vapor pressure (SVP). Fits at small t of the powerlaw

$$R = R_0 t^x \quad (7)$$

to data at all pressures where measurements exist (Tam, 1986) (0.05, 6.85, 14.73, 22.30, and 28.00 bar) yielded exponents which could, within their uncertainty, be represented by

$$x = 0.4395 - 0.000994P \quad (8)$$

where P has the units bar. Fits of the data with the exponent fixed at that given by Eq. 8 gave $R_0 = 0.00831, 0.00974, 0.01107, 0.01302, \text{ and } 0.01498$ cm K s / erg for the five isobars. In the calculations of finite-size and gravity effects given below we use x as given by Eq. 8 and R_0 given by linear interpolation between the values given here.

B. Resistivity of ^4He in 1- μm radius GCAs

The results of KA for the resistivity of ^4He at SVP in GCAs with capillary radii of 1 μm are shown in Fig. 3. The solid circles are the TA bulk data, and the open ones are the results for the finite geometry. As T_λ is approached, the finite-size effect becomes apparent. The data for the restricted geometry do not vanish at T_λ like the bulk data, and instead remain finite as t becomes negative.

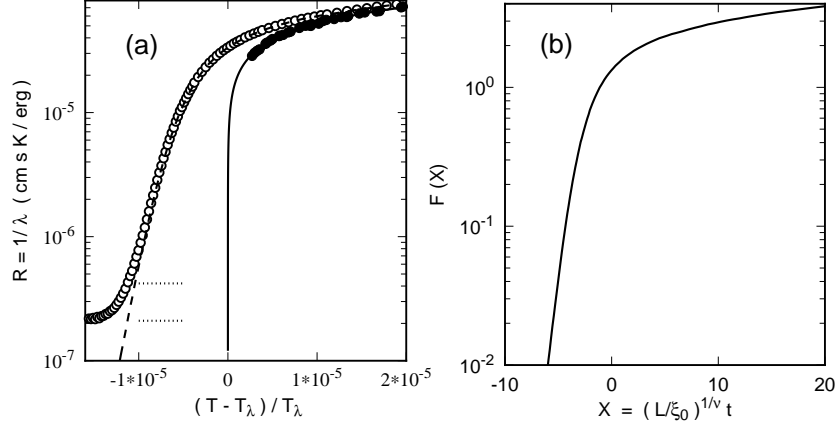


FIG. 3. (a): The thermal resistivity R at SVP for bulk helium (solid circles) and for helium in a GCA with pore radii of 1 μm (open circles). The solid line is the fit of Eq. 7 to the bulk resistivity. The dashed line is $R(t, L)$ after subtraction of the boundary contribution. (b): The scaling function $F(X)$ derived from the data in (a).

In order to compute the scaling functions from the experimental data and Eq. 4, we need the amplitudes ξ_0 of the correlation length above T_λ . The only direct experimental information about ξ_0 comes from the superfluid density below T_λ which gives the transverse correlation-length amplitudes ξ_0^T . (Singsaas, 1984; Greywall, 1972 & 1973) With the theoretical value of the universal ratio ξ_0/ξ_0^T this yields the amplitudes $\xi_0 = 1.432 \times 10^{-10}$ m at SVP and 1.314×10^{-10} m at $P = 28$ bar. Thus for the 1 μm capillaries at SVP we have $L/\xi_0 = 7 \times 10^3$. Figure 3b shows $F(X)$ computed from the KA data. Corresponding predictions of $R(t, L)$ for several values of L are shown in Fig. 4.

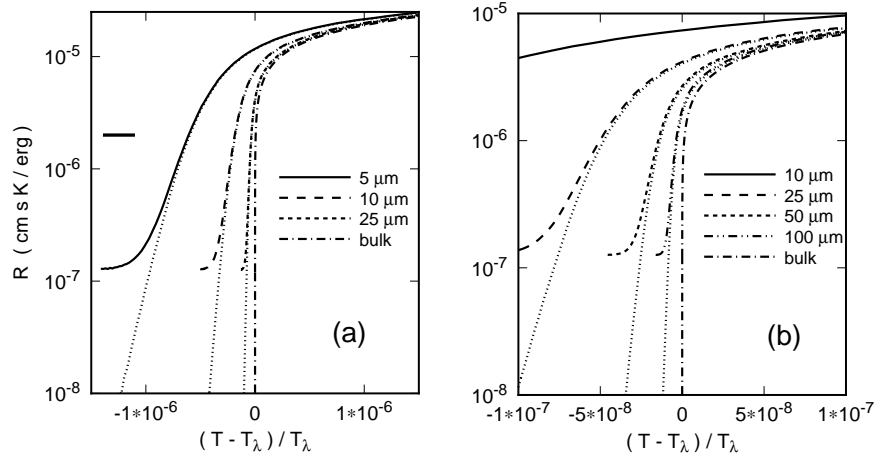


FIG. 4. Estimates based on the scaling function $F(X)$ of the thermal resistivity $R(t, L)$ of ^4He at SVP in cylindrical tubes of the various radii L given in the figure. The dotted lines show the predictions after correction for the boundary contribution. The horizontal bar in (a) shows the width of the two-phase region for a sample height $h = 5$ mm. On the scale of (b) this two-phase region would be wider than the figure.

V. QUANTITATIVE EVALUATION OF THE GRAVITY EFFECT

Here we present a quantitative estimate of the effect of gravity for various cylinder radii and pressures. To a reasonable approximation one can assume that the sample locally has bulk properties which are determined by a height dependent transition temperature $T_\lambda(z)$ and the local temperature $T(z)$. In this local approximation the average resistivity $\bar{R}(L, \bar{t})$ can be obtained by numerical integration over the sample height.

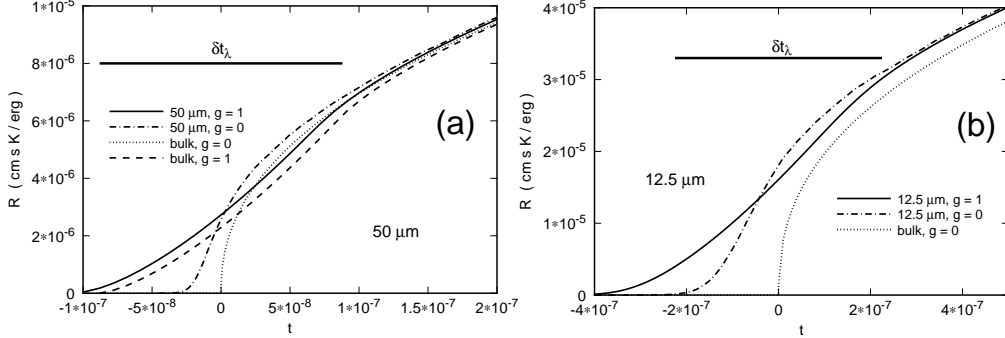


FIG. 5. (a): Estimates of the resistivity for a sample at SVP, of height $h = 3$ mm, for bulk helium and with $L = 50\mu\text{m}$, in the presence of gravity ($g = 1$) and for $g = 0$. The horizontal bar shows the width δt_λ and location of the two-phase region for bulk helium. (b): Same as (a), but for $P = 28$ bar and $L = 12.5\mu\text{m}$.

We consider the case where a constant heat current per unit area Q passes through the sample from the bottom. For illustrative purposes we used a sample height $h = 3$ mm, which is a convenient size (Kahn, 1995) for ground-based measurements. We chose $z = 0$ at the top and $z = h$ at the bottom of the sample. For a fixed temperature T_0 at the top, the temperature $T(z)$ was computed by numerical integration of $dT = -QRdz$ using $R = R(L, t(z))$ where $t(z) = (T(z) - T_\lambda(z))/T_\lambda$. The final temperature difference ΔT across the sample was used to compute $\bar{R} = \Delta T/(-Qh)$. The result was assigned to a reduced temperature $\bar{t} = (T_0 + \Delta T/2 - T_\lambda(h/2))/T_\lambda$. With these choices, we have $\bar{t} = 0$ when, for bulk helium and $Q = 0$, the interface between He-I and He-II is located at $z = h/2$. The calculation includes both the gravity effect and “curvature effects” (Tam, 1985) due to using a finite current. For the present calculations $Q = 10^{-10}$ W/cm² was used and curvature effects were negligible. In an actual experiment Q is likely to be larger, and curvature corrections may be required.

In Fig. 5a the results at SVP are shown for $L = 50\mu\text{m}$ in the presence of gravity and for $g = 0$. As a reference, the results for bulk helium are shown as well. The width δt_λ of the two-phase region is given by the horizontal bar. We see that for $L = 50\mu\text{m}$ gravity is the major “rounding” effect and the finite-size effect of interest is much smaller. Results for $P = 28$ bar and $L = 12.5\mu\text{m}$ are shown in Fig. 5b.

In order to quantify the extent of the gravity effect, we define the parameter

$$\Gamma^2(L, P) = \frac{\int_{-t_\lambda/2}^{t_\lambda/2} [R_g(t, L) - R_0(t, L)]^2 dt}{\int_{-t_\lambda/2}^{t_\lambda/2} R_0^2(t, L) dt} \quad (9)$$

where R_g and R_0 are the resistivity in the presence of gravity and for $g = 0$ respectively. We find that $\Gamma(P) \equiv \Gamma(\infty, P) \simeq 0.278$ regardless of P . In Fig. 6a we show $\Gamma(L, P)/\Gamma(P)$ as a function of L for three different pressures. We divide the $P - L$ plane into two regions, one in which gravity is relatively unimportant and another in which gravity has a dominating influence on the experiment. The criterion is naturally somewhat arbitrary. We chose the line where $\Gamma(L, P)/\Gamma(P)$ reaches 20 % of its value for the bulk system (another choice would merely move the boundary by a small amount). This boundary is

shown in Fig. 6b as a dashed line. One can see that by this criterion at SVP the gravity effect becomes important for $L > 17\mu\text{m}$, whereas for $P = 30$ bar it already becomes important near $L = 7\mu\text{m}$.

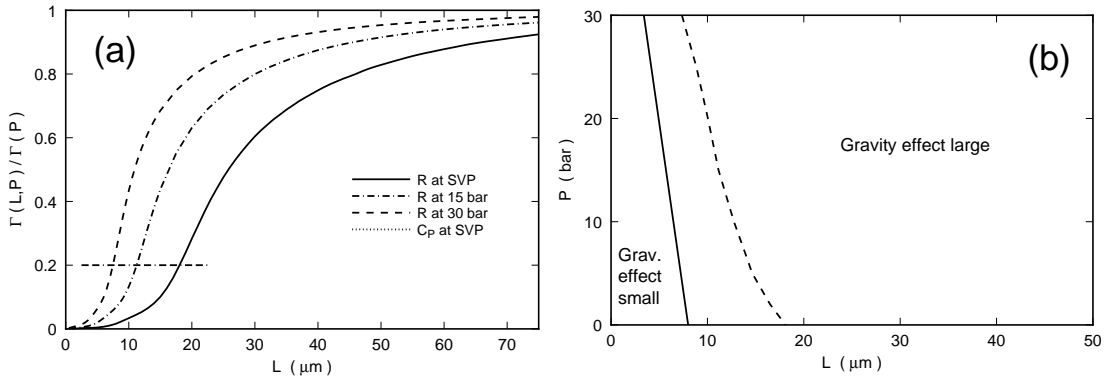


FIG. 6. (a): The parameter $\Gamma(L,P)/\Gamma(P)$ defined by Eq. 9 as a function of L for three different pressures. (b): Summary of the gravity effect as a function of P and L . To the left of the solid line, the gravity effect is relatively small and Earth-based measurements are feasible. To the right of the solid line microgravity experiments are necessary.

Closer inspection of the gravity effect reveals that the criterion in terms of Γ is misleading at low T where the resistivity decays exponentially. The reason for this is the exceptionally rapid variation of the exponential function which produces a large effect in the integration over the sample height. A criterion suitable in this temperature range (which will not be discussed here) yields the solid line in Fig. 6b. We see that at SVP gravity becomes of major importance for $L > 8\mu\text{m}$. At the highest pressure of 30 bar, this border is located at the rather small value $L \simeq 3.5\mu\text{m}$.

VI. PLANS FOR MICROGRAVITY EXPERIMENTS

On the basis of ground-based work, it is known that measurements of $R(L, t)$ along a single isobar can be completed in five to ten days. Several isobars would require one to three months, depending on the details of the measurements. Thus, BEST can be implemented in two ways, depending on flight opportunities. A set of measurements at saturated vapor pressure could be made during a Shuttle flight. This would provide an important test of finite-size scaling with respect to the size L , but would not address the issue of whether the scaling function is universal in the sense that it is pressure independent. Measurements along several isobars would address this latter issue, but would require two to three months and will be conducted only if a flight opportunity on the ISS becomes available. Present plans anticipate that BEST will have an opportunity to utilize the Low Temperature Microgravity Physics Facility (LTMPF) on the JEMF of the ISS in 2004.

REFERENCES

- Ahlers, G., *Phys. Rev.* **171**, 275 (1968); *J. Low Temp. Phys.* **84**, 173 (1991).
 See, for instance, Dohm, V., *Phys. Script.* **T49**, 46 (1993).
 See, for instance, Fisher, M. E., in *Critical Phenomena*, Proc. 51st "Enrico Fermi" Summer School, Varenna, edited by M. Green, Academic, NY, 1971, p. 1.
 Goldner, L. S., and Ahlers, G., *Phys. Rev. B* **45**, 13129 (1992).
 Greywall, D. S., and Ahlers, G., *Phys. Rev. Lett.* **28**, 1251 (1972); *Phys. Rev. A* **7**, 2145 (1973).
 Kahn, A. and Ahlers, G., *Phys. Rev. Lett.* **74**, 944 (1995).
 Singaas, A., and Ahlers, G., *Phys. Rev. B* **30**, 5103 (1984).
 Tam, W. Y., and Ahlers, G., *Phys. Rev. B* **32**, 5932 (1985).
 Tam, W. Y., and Ahlers, G., *Phys. Rev. B* **33**, 183 (1986).